Lab on a Chip

Cite this: *Lab Chip*, 2012, **12**, 4059–4062

www.rsc.org/loc

TECHNICAL INNOVATION

Microchannel refill: a new method for fabricating 2D nanochannels in polymer substrates

Jing-min Li,[a] Chong Liu,*[ab] Xue Ke,[a] Zheng Xu,[a] Ya-jie Duan,[a] Yan Fan,[a] Meng Li,[a] Kai-ping Zhang[a] and Li-ding Wang[ab]

Received 21st December 2011, Accepted 21st June 2012
DOI: 10.1039/c2lc40078b

In this paper, we present a new approach that is capable of fabricating nanochannels in a poly(methyl methacrylate) (PMMA) substrate. This method, which we call microchannel refill (MR), utilizes the refilling of glassy thermoplastics under thermal compression to reduce a microscopic channel to a nanochannel. It only has two main steps. First, a microchannel is fabricated in a PMMA substrate using normal hot embossing. Second, the microchannel is compressed under a certain temperature and pressure to obtain a nanochannel. We show that a nanochannel with a width as small as 132 nm (with a depth of 85 nm) can be easily produced by choosing the appropriate compression temperature, compression pressure, original microchannel width and original microchannel aspect ratio. Compared with most current nanochannel fabrication methods, MR is a quick, simple and cost-effective way to produce nanochannels in polymer substrates.

1. Introduction

Fabricating nanoscale channels in a polymer substrate is significant for the research in nanofluidics.[1] Conventional techniques can obtain nano-features using some state-of-the-art facilities. However, these techniques are not widely accessible due to their high cost.[2] A number of recently developed methods, such as nanoimprinting[3,4] and soft lithography,[5,6] utilize a mold or a stamp with nanopatterns to replicate the features into a substrate by conformal contact. Though they give the possibility of fabricating nanopatterns with large areas and high throughput, to obtain a low cost mold with the required nano-features may be still a problem.[7] Self-organization, which involves no complicated equipment, is attractive in nanochannel fabrication, but the instability in obtained homogenous nanochannels still requires further study.[8]

By contrast, several nanochannel fabrication approaches based on microchannel-reduction represent alternatives. Chemical shrink utilizes the cross-linking reaction of a photoresist to reduce the size of the microchannel to nanoscale.[9,10] This method requires a special photoresist and cannot be used in a normal polymer. Thermal reflow utilizes the flow of melt-state SU-8 to reduce the size of a microchannel to several tens to several hundreds of nanometers.[11,12] This approach, due to its instability in obtaining homogenous nanochannels, may be problematic in many applications. Mechanical drawing utilizes a tensile test machine to draw a microchannel to nanoscale.[13] Due to the form of the neck-down region during the drawing process, the fabricated substrate, which contains the nanochannel, always has a dumb-bell-like shape which may meet limited applications. In addition, this method can only produce straight nanochannels.

In this paper, we demonstrate a new approach, which we call microchannel refill (MR), to produce nanochannels in a PMMA substrate. The procedure of MR is schematically illustrated in Fig. 1. Initially, a mold with microscale protrusions, which is produced by electroforming and has a line-width of several tens of microns, is utilized to fabricate microchannels in a PMMA substrate using common hot embossing. Then, the fabricated substrate is compressed under a certain temperature and pressure. During the compression process, the glassy state PMMA will refill the microchannel and reduce its size to nanoscale. The MR method requires no nanoscale masks, nanoscale stamps (or molds), complicated lithography process, special polymer or expensive equipment. It is a low cost and simple 2D nanochannel fabrication method, which can be readily performed.

2. Experimental

2.1 Materials

The commercial PMMA plates used here, with a glass transition temperature (T_g) of 105 °C, are provided by Asahi Kasei Corporation. Their thicknesses are all 1 mm, and the contact angles are 76.4°. Each plate is cut into 20 mm × 20 mm substrates for hot embossing and compression experiments.

2.2 Hot embossing of the original microchannels

The detailed hot embossing procedures are as follows. Firstly, the mold and the PMMA substrate are heated to 90 °C and 100 °C,

[a]*Key Laboratory for Micro/Nano Technology and System of Liaoning Province, Dalian University of Technology, Dalian 116023, P. R. China. E-mail: chongl@dlut.edu.cn; Tel: +86 0411 84707946*
[b]*Key Laboratory for Precision and Non-traditional Machining Technology of Ministry of Education, Dalian University of Technology, Dalian 116023, P. R. China*

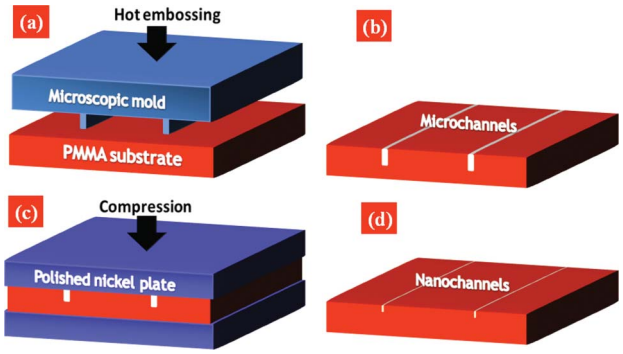

Fig. 1 Procedure of the MR method: (a) and (b) using a microscopic mold to replicate microchannels into a PMMA substrate using hot embossing; (c) and (d) utilizing two polished nickel plates to compress the microchannel to nanoscale at a temperature near T_g of the PMMA material.

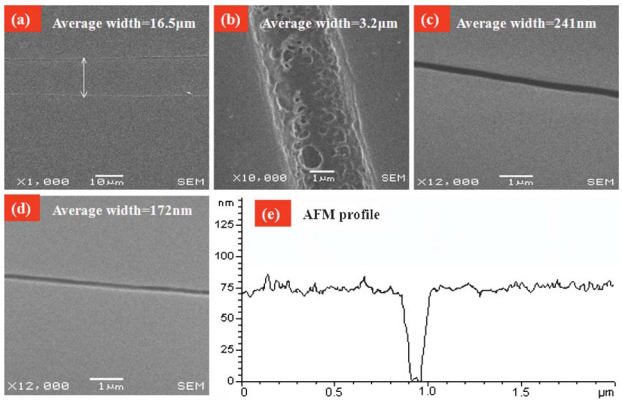

Fig. 2 The effects of compression temperature and compression pressure on channel reduction. (a) A channel is compressed to 16.5 μm wide and 170 nm deep under 117 °C and 8 MPa conditions. (b) A channel is compressed to 3.2 μm wide and 230 nm deep under 109 °C and 8 MPa conditions. Figure (a) and (b) show that the size reduction in channel depth is faster than that in channel width at a temperature above T_g. (c) A fabricated nanochannel of 241 nm wide and 130 nm deep, which is obtained under 103 °C and 8 MPa conditions. This image indicates that more homogeneous reduction in channel depth and width can be obtained at a temperature below T_g. (d) A 172 nm wide nanochannel obtained under 103 °C and 9 MPa compression conditions. (e) The cross-sectional profile of the 172 nm-wide nanochannel, which is obtained using AFM.

and kept for about 2 min to 3 min in order to improve the uniformity of the temperature distribution. Secondly, the mold and the substrate are heated to 110 °C and 125 °C. At the same time, the substrate is pressed by a mold with micro-protrusions. The embossing pressure is about 1.5 MPa. Thirdly, the temperature and the pressure are maintained for about 3 min–5 min. Finally, the substrate is cooled and de-molded as the temperature decreases to about 60 °C.

3. Results and discussion

The reduction of a microchannel will be affected by compression temperature, compression pressure, width of the original microchannel and the aspect ratio of the original microchannel.

3.1 Compression temperature and pressure

We use a pressure of 8 MPa to compress microchannels 20 μm-wide, 20 μm-deep and 2 mm-long at 85 °C–120 °C. The temperature ramp rate is about 0.5 °C s^{-1}. The pressure is applied by using a rate of approximately 0.04 MPa s^{-1}. Fig. 2a and b show the SEM images of the fabricated nanochannels obtained at 117 °C and 109 °C, respectively. At 117 °C, the average channel width, which is the average of the channel widths at ten different positions, only decreases to 16.5 μm when the channel depth has been reduced to approximately 170 nm (measured by a surface profiler, Surfcoder ET-4000M). At 109 °C, the average channel width decreases to 3.2 μm when the channel depth has reduced to 230 nm. At this temperature scale, the reduction of channel depth is faster than that of the channel width. Only planar nanochannels (1D) can be obtained. In contrast, it is found that the reductions in channel depth and channel width are more homogeneous as the compression is performed at a temperature below T_g. Fig. 2c shows the fabricated nanochannel obtained at 103 °C. As the channel depth decreases to 130 nm, the average channel width exhibits an obvious reduction to 241 nm. [The depth of a 2D nanochannel is measured by atomic force microscopy (AFM)].

The reason for this phenomenon is not clear at the moment. We think that it may be attributed to the size effect. It is well-known that, under a longitudinal compression, the deformation in the lateral direction is mainly caused by a lateral squeezing force.[14] The value of the squeezing force will be mainly determined by the material bulk modulus, which will vary to follow the change in temperature and size. Some mechanical tests performed in recent decades, such as micro/nano indentation (or scratch), have indicated that there is an increase in the mechanical properties of a material as the scale decreases near 1 μm.[15,16] As the temperature increases above T_g, the PMMA material exhibits a hyperelastic state. Its bulk modulus dramatically decreases 100 to 1000 fold.[17] Hence, the lateral squeezing force (or stress) whose value is mainly determined by the bulk modulus will obviously decrease. Considering the increase in partial modulus and rigidity near the microchannel as the line-width decreases to 1 μm, the squeezing force is not enough to squeeze the polymer into the microchannel to reduce its size below 1 μm. In contrast, at a temperature below T_g, the bulk modulus and rigidity is closer to those at the microchannel region. Hence, the squeezing force will be large enough to compress the width of the microchannel below 1 μm.

At a temperature of 103 °C–105 °C, to increase the compression pressure to 9 MPa–10 MPa can further reduce the size of a fabricated nanochannel. Fig. 2d shows the SEM image of a fabricated nanochannel, which is obtained under 103 °C and 9 MPa conditions. It can be seen that the average width of the fabricated nanochannel has been further reduced to approximately 172 nm. Its cross-sectional profile is shown in Fig. 2e. If the pressure is increased to 11–12 MPa, though the width of the fabricated nanochannel will be further reduced (may be near 100 nm), polymer crazes,[18] which may cause irregular deformation of material at a partial region, are observed near the edges of the channel. Due to the effects of polymer crazes, the edges of the fabricated nanochannel become discontinuous. As the temperature decreases below 100 °C, to compress the microchannel

below 1 μm becomes very difficult even using a pressure of 13 MPa–14 MPa.

3.2 The width of the original microchannel

The width of the original microchannel is another factor which can affect channel reduction. Here, we perform three compression experiments to test its effects. The microchannels used in these three experiments have widths of 140 μm, 75 μm and 15 μm, respectively. To simplify the study, these microchannels all have been fabricated with an aspect ratio of 1, and the compressions were all performed under 103 °C and 9 MPa conditions. The temperature ramp rate and the pressure increase rate are 0.5 °C s^{-1} and 0.04 MPa s^{-1}, respectively. We use the 3σ-line-width roughness (LWR), [19] which is the stochastic variation in width that occurs along the length of a line to test the shape variation of a fabricated nanochannel. This can clearly show the effects of the original width on channel reduction. For the 140 μm-wide microchannel, the MR process has reduced its average width to approximately 715 nm (Fig. 3a). But the 3σ-LWR has reached 480.6 nm, which indicates that the fabricated channel has a dissatisfactory shape. For the 75 μm-wide microchannel, the 3σ-LWR of the fabricated nanochannel is 98.5 nm when its size has been reduced to 552 nm. For the 15 μm-wide microchannel, the compression result is shown in Fig. 3b. The average width of the fabricated nanochannel is 132 nm. The depth of the nanochannel is about 85 nm and the 3σ-LWR has been reduced to 17.2 nm.

Considering the 3σ-LWR of the fabricated nanochannel shown in Fig. 2d, whose original width is 20 μm, a relationship between the width of the original microchannel and the 3σ-LWRs of the fabricated nanochannel can be established (Fig. 3c). It can be seen that the 3σ-LWR value will rise to follow the increase in microchannel original width. Hence, reducing microchannel original width can enhance the quality of the fabricated nanochannel. The dissatisfactory shape of the fabricated nanochannel as the original microchannel width is large (especially larger than 100 μm) may be caused by the effects of compression rate (defined as $S_{initial}/S_{final}$, where $S_{initial}$ is the original size, S_{final} is the compressed size).[20] The compression rate is approximately 196 when a microchannel is compressed from 140 μm to 715 nm. It has been reported that, at a high compression rate, the deformation behavior of thermoplastics will be affected by the defects and the microstructures of the material and exhibit irregular or heterogeneous character.[21] This heterogeneous deformation may cause a dissatisfactory channel shape. The relationship between compression rate and the 3σ-LWR has also been studied (Fig. 3d). It is also found that the increase in compression rate will result in the rise of the 3σ-LWR.

3.3 The aspect ratio of the original microchannel

The aspect ratio of the original microchannel is another issue. The results for an aspect ratio of 1 have been discussed above. Here, we fabricate the other three types of straight microchannels with original aspect ratios of 0.55, 0.72 and 2.1, respectively. We use these microchannels to test the effects of the original aspect ratio. To simplify the study, the compressions are all performed under 103 °C and 9 MPa conditions. The temperature ramp rate and the pressure increase rate are 0.5 °C s^{-1} and 0.04 MPa s^{-1}, respectively. For the microchannel with an aspect ratio of 0.55, the compression result is shown in Fig. 4a. It is found that the average width of the microchannel only decreases to approximately 1.5 μm as its depth has been reduced to 520 nm. For the microchannel with an aspect ratio of 0.72, the compression result is shown in Fig. 4b. The average width of the microchannel has been compressed to approximately 1.2 μm

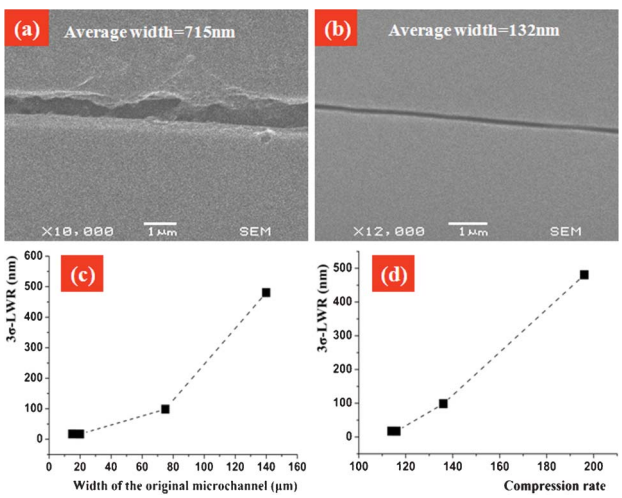

Fig. 3 The effect of original microchannel width on channel reduction. (a) A fabricated nanochannel whose original width is 140 μm. (b) A fabricated nanochannel whose original width is 15 μm (c) The relationship between original microchannel width and the 3σ-LWR, which indicates that reducing the original width can increase the quality of a fabricated nanochannel. (d) The relationship between compression rate and 3σ-LWR value, which indicates that the 3σ-LWR will increase as the compression rate rises.

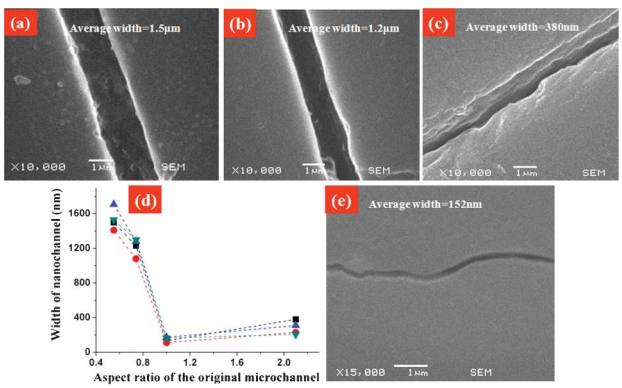

Fig. 4 The effect of the aspect ratio of the original microchannel on channel reduction. (a) The compression result of the channel with an original aspect ratio of 0.55. The channel has only been reduced to 1.5 μm wide. (b) The fabricated channel whose original aspect ratio is 0.72. Its average width is only 1.2 μm. (c) A nanochannel obtained by compressing a microchannel with an original aspect ratio of 2.1. It has a serpentine line-shape and uneven morphology and its average width is 380 nm. (d) A profile to exhibit the relationship between the original aspect ratio and the width of the fabricated nanochannel. The increase in width for the original aspect ratio above 1 may be caused by stress concentration and strain hardening. (e) A serpentine nanochannel fabricated by using the MR method, whose average width is 152 nm.

as its depth decreases to 580 nm. For the microchannel with an aspect ratio of 2.1, the compression result is shown in Fig. 4c. The fabricated nanochannel is 380 nm wide and 210 nm deep. The zigzag edges can be clearly seen and its 3σ-LWR has reached 101.4 nm.

The above experiments have been repeated four times. According to the results, considering the conditions for the original aspect ratio of 1, a relationship between the original aspect ratio and the fabricated nanochannel width can be established. Fig. 4d shows the profile. It can be seen that the width of the fabricated channel will decrease as the original aspect ratio increases from 0.55 to 1. As the original aspect ratio increases above 1, there is a tendency for the width of the fabricated channel to rise. The reason for this phenomenon still needs to be investigated. We think it may be caused by stress concentration and strain hardening induced by the irregular deformation of the polymer around the channels. As is shown in Fig. 4c, the shape of the fabricated nanochannel becomes severely zigzag and the surface morphology around the channel becomes uneven when the aspect ratio increases to 2.1. According to plasticity theory, the changes in shape and morphology may induce stress concentration at the partial regions of the channel.[22] The stress concentration will induce strain hardening at these regions which will limit the deformation of the material and result in the difficulty in channel reduction. In contrast, as is shown in Fig. 2d and Fig. 3b, the line-shape and the morphology of the channels with an original aspect ratio of 1 is straighter and flatter. The effects of stress concentration and strain hardening may be slight.

We have shown that straight nanochannels can be fabricated on a PMMA substrate using MR methods. The nanochannels with other shapes can also be obtained using this method. Fig. 4e shows a serpentine nanochannel fabricated using the MR method. Its average width is approximately 152 nm. The nanochannel is fabricated under 103 °C and 9 MPa conditions. The width and aspect ratio of the original microchannel are 15 μm and 1, respectively.

4. Conclusions

The MR method presented in this work shows that nanochannels can be produced from a microscopic mold and a simple compression process without using special polymers, nano-masks or nano-molds. In fact, there are only two main steps in the MR method. First, the microfeatures on a mold are replicated into a polymer substrate using hot embossing. Second, the fabricated microchannel is compressed to nanoscale under a certain temperature and pressure. For the PMMA material used here, the optimal compression temperature and pressure are 103 °C–105 °C and 8 MPa–9 MPa. The optimal width of the original microchannel is below 20 μm. The optimal aspect ratio of the original microchannel is 1. The MR method is well controlled and highly reproducible. It can also be used to fabricate nanochannels in other thermoplastic materials. In future studies, this method can be used in combination with other approaches, such as electroforming and casting, to produce nano-protrusion features on metal surfaces or PDMS surfaces.

Acknowledgements

This work is supported by the National Natural Science Foundation of China (91023017; 51105060; 20890024; 91023046), The National High Technology Research and Development Program of China (No: 2012AA040406), the National Basic Research Program of China (No: 2007CB714502) and the China Postdoctoral Science Foundation (20100481237; 201104601).

References

1 R. Chantiwas, S Park, A. S. Steven, B. C. Kim, S. Takayama, V. Sunkara, H. Hwang and Cho. Yoon-Kyoung, *Chem. Soc. Rev.*, 2011, **40**, 3677–3702.
2 Hao-Li Zhang, G. B. David and D. Alexandre, *Nano Lett.*, 2004, **4**(8), 1513–1519.
3 Se Hyun Ahn and L. Jay Guo., *ACS Nano*, 2009, **3**(8), 2304–2310.
4 S. Ducharme and G. Alexei, *Nat. Mater.*, 2009, **8**, 9–10.
5 M. H. Lee, D. H. Mark, W. Zhou, J.-C. Yang and W. O. Teri, *Nano Lett.*, 2011, **11**(2), 311–315.
6 Zhiwei Li, Yanni Gu, Lei Wang, Haixiong Ge, Wei Wu, Qiangfei Xia, Changsheng Yuan, Yanfeng Chen, Bo Cui and R. Stanley Williams., *Nano Lett.*, 2009, **9**(6), 2306–2310.
7 D. G. Byron, Qiaobing Xu, M. Stewart, D. Ryan, C. Grant Willson and M. W. George, *Chem. Rev.*, 2005, **105**, 1171–1196.
8 Mann. Stephen, *Nat. Mater.*, 2009, **8**, 781–792.
9 T. Kanda, H. Tanaka and K. Yager, *Microlithography world*, 1999, **8**(4), 26–27.
10 T. Ishibashi, T. Toyoshima, N. Yasuda and T. Kanda, *Jpn. J. Appl. Phys.*, 2001, **40**, 419–425.
11 C. C. Meng, G. R. Liao and S. S. Lu, *Electron. Lett.*, 2001, **37**, 1045–1046.
12 Hsuen-Li CHEN, Fu-Hsiang KO and L. Lung-Sheng, *Jpn. J. Appl. Phys.*, 2002, **41**, 4163–4166.
13 P. Sivanesan, K. Okamoto, D. English, S. L. Cheng and L. D.. Don, *Anal. Chem.*, 2005, **77**(7), 2252–2258.
14 J. Roesler, H. Harders and B. Martin, *Mechanical Behaviour of Engineering Materials, Metals, Ceramics*, Polymers and Composites, Springer, 2006.
15 B. D. Beake and G. A. Bell, *Witold Brostow and Wunpen Chonkaew. Polymer International*, 2007, **56**, 773–778.
16 K. Rashid, Abu Al-Rub and Abu N. M. Faruk, *Int. J. Mater. Struct. Integr.*, 2010, **4**, 251–277.
17 E. M. James, *Physical properties of polymers handbook. 2nd ed.*, Springer, 2007.
18 J. Rottler and O. R. Mark, *Phys. Rev. Lett.*, 2002, **89**, 195501.
19 Y. C. Stephen and Xia. Qiangfei, *Nat. Nanotechnol.*, 2008, **3**, 295–300.
20 A. D. Mulliken and M. C. Boyce, *Int. J. Solids Struct.*, 2006, **43**(5), 1331–1356.
21 C. M. Roland, J. N. Twigg and Y. Vu, *Polymer*, 2007, **48**(2), 574–578.
22 *Vahram Hakobyan. Stress concentration near defects in homogeneous and compound bodies*, Lap Lambert Academic Publishing, 2011.

